ELSEVIER

Journal of Luminescence 87–89 (2000) 1192–1195

JOURNAL OF LUMINESCENCE

www.elsevier.com/locate/jlumin

Time-resolved micro-photoluminescence of epitaxial laterally overgrown GaN

A. Kaschner[a,*], J. Holst[a], A. Hoffmann[a], I. Broser[a], P. Fischer[b], F. Bertram[b], T. Riemann[b], J. Christen[b], K. Hiramatsu[c], T. Shibata[d], N. Sawaki[d]

[a]*Institut für Festkörperphysik, TU Berlin, Hardenbergstraße 36, 10623 Berlin, Germany*
[b]*Institut für Experimentelle Physik, Otto-von-Guericke-Universität, P.O. Box 4120, 39016 Magdeburg, Germany*
[c]*Department of Electrical and Electronic Engineering, Mie University, Mie 514-8507, Japan*
[d]*Department of Electronics, Nagoya University, Nagoya 464-01, Japan*

Abstract

Epitaxial laterally overgrown GaN (ELOG) structures are microscopically characterized using cathodoluminescence (CL), micro-Raman spectroscopy and time-resolved micro-photoluminescence. Two ELOG samples consisting of a 3 μm thick GaN buffer layer on (0 0 0 1) sapphire masked with SiO_2 stripes parallel to $\langle 1\,\bar{1}\,0\,0\rangle$ and $\langle 1\,1\,\bar{2}\,0\rangle$ direction, respectively, were investigated. Beside their technological relevance ELOG samples are a superior subject of investigations due to internal gradients in strain and free carrier concentration. To study the influence of the different lateral growth mechanisms on the optical properties of the GaN in the coherently grown and in the overgrown region, we correlate the temporal behavior of the near band gap luminescence with the local free carrier concentration as determined by the peak position of the coupled phonon plasmon modes (LPP). The spatial resolution of both of the microscopic methods is about 1 μm. As a result we observe distinct differences in the decay times of the near band gap luminescence for the two different samples as well as for different regions within one sample. The observed behavior is explained by the fact that extrinsic or intrinsic defects give rise to shallow donor levels, causing a gradient in free carrier concentration. Therefore the near-band-gap emission changes from excitonic luminescence to band-to-band recombination depending on the distance from the interface as evidenced by micro-photoluminescence. Beside these drastic changes we also observe a change in decay times in the region of excitonic emission correlated with the donor concentration which leads to a different influence of the coulomb screening effect.

PACS: 78.20. − e; 78.30.Fs; 78.60.Hk

Keywords: ELOG; Time-resolved micro-PL; Excitonic luminescence; Micro-Raman spectroscopy

The group-III nitrides and its related ternary alloys have been growing to the most promising material for light emitting diodes and laser diodes in the UV and blue spectral range, for a review see [1]. Recently, laser diodes with an estimated lifetime of more than 10 000 h were reported and are now available commercially [2]. To achieve such lifetimes necessary for commercial application the introduction of the epitaxial lateral overgrowth (ELO) technique was claimed to be effective. This method has already been applied successfully in reducing dislocation density by at least 3–4 orders of magnitude compared to that of hetero-epitaxial GaN on sapphire (approx. $10^{10}\,cm^{-2}$) [3,4]. It was shown that lateral overgrowth of GaN leads to a direct improvement of quality of the InGaN multi-quantum well structures due to the elimination of dislocations [5].

The ELOG samples investigated here are schematically depicted in Fig. 1a and b. A 3 μm thick GaN layer was grown by metalorganic vapor-phase epitaxy

*Corresponding author. Fax: + 49-30-314-27705.
E-mail address: kaschner@physik.tu-berlin.de (A. Kaschner)

0022-2313/00/$ - see front matter
PII: S0022-2313(99)00593-1

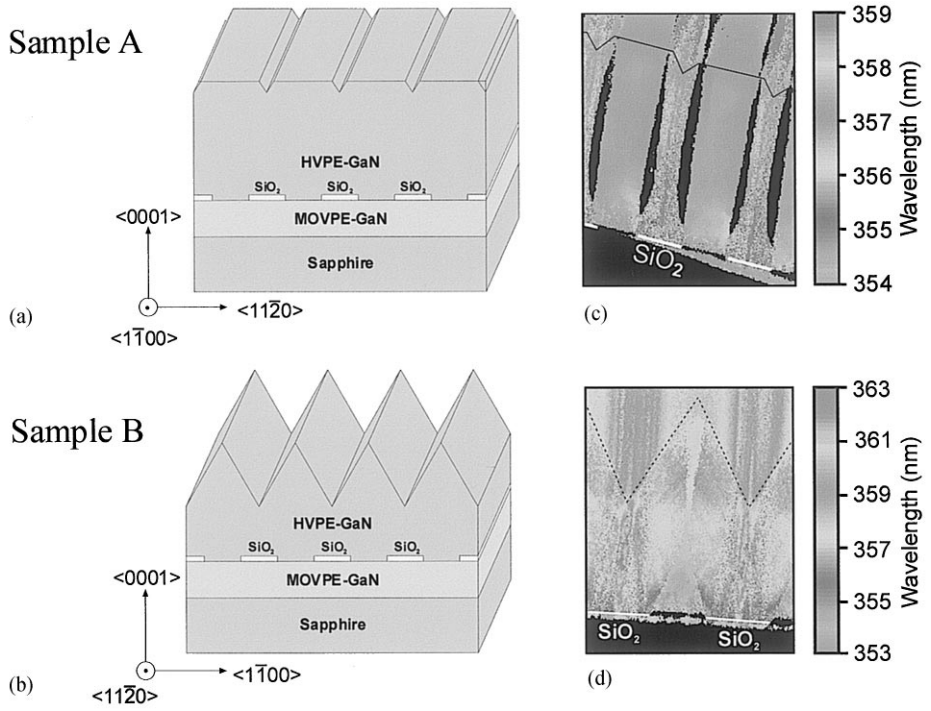

Fig. 1. Schematic structure of the ELOG samples A and B with the SiO_2 masks parallel to $\langle 1\,\underline{1}\,0\,0\rangle$ direction (a) and $\langle 1\,1\,\underline{2}\,0\rangle$ direction (b) together with the two corresponding CL wavelength images (c,d) taken at 5 K. One can clearly distinguish between the coherently grown and the overgrown regions in both samples.

(MOVPE) on a (0 0 0 1) sapphire substrate and patterned with 120 nm thick SiO_2 masks parallel to the $\langle 1\,\underline{1}\,0\,0\rangle$ (sample A) and $\langle 1\,1\,\underline{2}\,0\rangle$ (sample B) direction. The width of the openings and the stripes are 10 μm each. This structure was subsequently overgrown with a 50 μm thick GaN layer deposited by hydride vapor-phase epitaxy (HVPE) through the windows in the SiO_2 masks on the underlying MOVPE GaN layer. Details of growth are given elsewhere [6].

The setup for the micro-PL and cathodoluminescence experiments are described in Refs. [7,8], respectively. The micro-PL measurements at 4 K having a spatial resolution better than 600 nm were carried out in backscattering geometry using a glass fiber. The photoluminescence signal was analyzed in a 0.35 m subtractive double spectrometer and detected by a microchannel plate photomultiplier. For time-resolved measurements a single-photon counting setup was used with a 50 ps FWHM response to the laser pulse. Employing convolution techniques the overall time resolution is enhanced to 15 ps. A frequency-doubled dye laser pumped by a Nd : YAG was used for excitation. The Raman-scattering experiments at RT were carried out using a triple-grating spectrometer equipped with a confocal microscope optic. The excitation wavelength was 488 nm.

In Fig. 1c and d two cross-section cathodoluminescence images are shown. One can clearly distinguish between the coherently grown and the overgrown regions, i.e. window and mask region, respectively. The coherently grown region of sample A exhibits a uniform monochromatic rectangle up to the surface where a sharp luminescence of the neutral donor-bound exciton at 357.6 nm dominates the spectra, whereas for sample B a triangle of excitonic luminescence of approximately 10 μm in height is formed. In the area on top of the SiO_2 masks, i.e., in the coalescence region, the luminescence is strongly red-shifted, indicating the strong impact of defect mediated effects. In the following we present results of time-resolved micro-photoluminescence and micro-Raman measurements for the two different regions of both samples. For a more detailed discussion of the CL results refer to Refs. [9,10].

In Fig. 2 the decay time of the near-band-gap emission and the local free carrier concentration as determined by the position of the LPP modes in the Raman spectra are shown as function of the distance from the substrate interface. The scans were performed right in the middle of the mask and the window region with a distance of a few microns between two adjacent data points. The decay time of the excitonic luminescence in the coherently

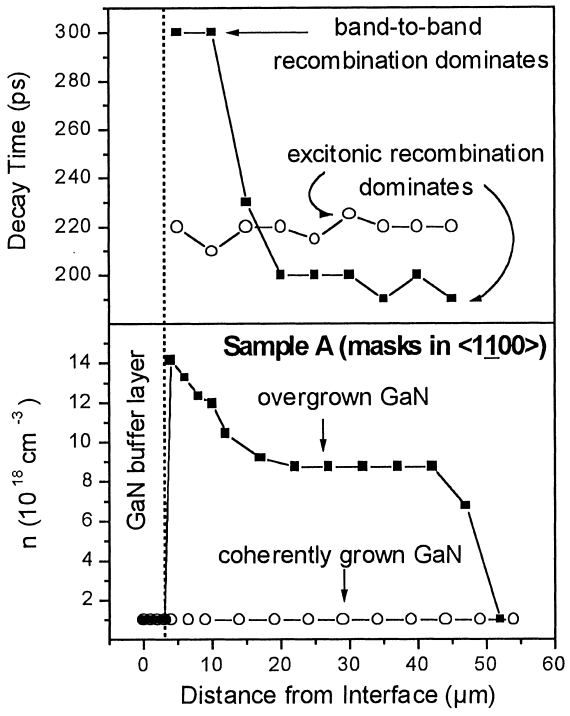

Fig. 2. Decay time of the near-band-gap emission (upper part) and free carrier concentration (lower part) as function of the distance from the substrate interface of sample A having the SiO_2 masks along $\langle 1\,\underline{1}\,0\,0\rangle$ direction. The data points are taken along a line from the interface to the surface in the coherently grown region (open circles) as well as in the overgrown (filled squares) region.

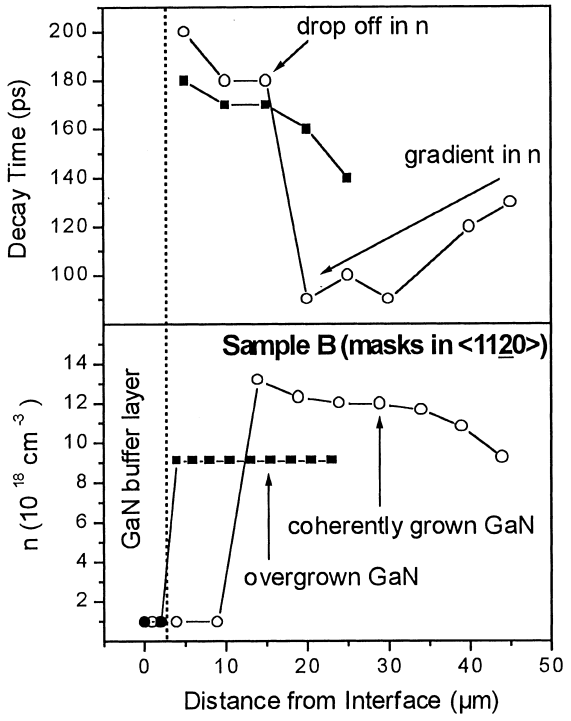

Fig. 3. Decay time of the near-band-gap emission (upper part) and free carrier concentration (lower part) as function of the distance from the substrate interface of sample B having the SiO_2 masks along $\langle 1\,1\,\underline{2}\,0\rangle$ direction. The data points are taken along a line from the interface to the surface in the coherently grown region (open circles) as well as in the overgrown (filled squares) region.

grown region (open circles) remains constant at 220 ps within the experimental accuracy. In this region the free electron concentration is below the detection limit of our method and all data points are set to $1\times10^{18}\,cm^{-3}$. In the overgrown region of sample A the time constants (solid squares) are almost constant with decreasing distance from the substrate but sharply increased from 200 to 300 ps at 10 μm above the masks. In the same region a jump in free carrier concentration from 9×10^{18} to $1.4\times10^{19}\,cm^{-3}$ occurs. Therefore, the temporal behavior can be understood, taking into account that the high free carrier concentration causes a change from excitonic to band-to-band recombination, which is evidenced by a broad luminescence on the high-energy side of the $D^{O}X$ in the micro-PL spectra and also found in CL spectra in this sample region [9,10]. As known from highly doped wide-gap semicondutors as CdS : In, a sharp increase to longer decay constants is observed above the Mott density [11]. This is because the band-to-band transition probability is smaller than the exciton transition probability, though slower decay times are expected.

The recombination dynamics of sample B is summarized in the upper part of Fig. 3. In the overgrown region the decay time is slightly increased from 140 to 180 ps as one approaches the substrate interface. Above the masks the transient is composed of the dynamics of band-to-band transitions and excitonic processes. The influence of band-to-band processes is reduced with distance from the masks and the faster excitonic processes dominate the decay. The free carrier concentration remains constant at $9\times10^{18}\,cm^{-3}$ in this region.

In the coherently grown region the decay time is reduced from 130 ps near the surface to 90 ps at 20 μm from the substrate with decreasing distance from the substrate. At 15 μm from the substrate a sharp increase to time constants of 200 ps is observed. This can be explained by an increased number of incorporated impurities, changing the free carrier concentration from 9×10^{18} to $1.3\times10^{19}\,cm^{-3}$ when moving towards the substrate. We think that like for other GaN samples [12] radiative processes dominate the decay of the donor-bound exciton in our samples. Following Rashba and Gurgenishvili [13] the average distance of impurity

centers compared to the exciton–impurity complex is reduced, when the number of impurities is increased. Thus, the higher the impurity concentration, the greater the Coulomb screening on the donor–exction binding energy. The effective binding energy is lowered and so is the radiative decay time, but the donor-bound exciton complex still exists. This drastically changes at 15 μm from the substrates. The sharp increase in time constant is linked to a drop off in free carrier concentration from 1.3×10^{19} to $1\times10^{18}\,cm^{-1}$, obtained by micro-Raman experiments at this point, within the experimental accuracy.

For the understanding of the influence of the growth mechanisms on the optical properties, Ref. [14] makes use of the fact that the vertical growth rates decrease, while the lateral overgrowth rates increase as the mask stripe orientation changes from $\langle 1\,1\,\underline{2}\,0\rangle$ to $\langle 1\,\underline{1}\,0\,0\rangle$. Therefore, the triangle appearing in the CL image of sample B with the masks along $\langle 1\,1\,\underline{2}\,0\rangle$ direction extends to form a rectangle for the $\langle 1\,\underline{1}\,0\,0\rangle$ ELOG structure (sample A). In both structures we find poor crystalline and optical properties in the overgrown, especially close above the SiO_2 masks.

Summarizing our results, we microscopically characterized two ELO GaN samples with different orientations of the SiO_2 masks in a comprehensive manner. From our findings we identified the different growth regimes: the coherently grown region of sample A (masks along $\langle 1\,\underline{1}\,0\,0\rangle$) shows perfect excitonic micro-luminescence, i.e. high crystallographic quality and low carrier concentration up to the surface. This is confirmed by long decay times of 220 ps which are almost unchanged along the cross section. In the ELOG sample B we observe a sharp decrease of the decay times from 180 to 90 ps above the low-impurity region which corresponds to the heights of the triangle in the CL image in Fig. 1d. Above this point the declining impurity concentration leads to a reduced exciton screening and longer time constants.

The drastic change of the time constant at 10 μm from the substrate interface in the overgrown region of sample A is explained by a change in the origin of the recombination from excitonic to band-to-band recombination. The influence of many-particle processes accounts for the carrier dynamics in the overgrown region of the $\langle 1\,1\,\underline{2}\,0\rangle$ sample as well.

Acknowledgements

A.K. acknowledges the support of an Ernst-von-Siemens-scholarship.

References

[1] S. Nakamura, G. Fasol, The Blue Laser Diode, Springer, Berlin, 1997.
[2] S. Nakamura, M. Senoh, S. Nagahama, N. Iwasa, T. Yamada, T. Matsushita, H. Kiyoku, Y. Sugimoto, T. Kozaki, H. Umemoto, M. Sano, K. Chocho, Jpn. J. Appl. Phys. Part 2 36 (1997) L1568.
[3] A. Usui, H. Sunakawa, A. Sakai, A. Yamaguchi, Jpn. J. Appl. Phys. Part 2 36 (1997) L899.
[4] H. Marchand, X.H. Wu, J.P. Ibbetson, P.T. Fini, P. Kozodoy, S. Keller, J.S. Speck, S.P. Den Baars, U.K. Mishra, Appl. Phys. Lett. 73 (1998) 747.
[5] S.F. Chichibu, H. Marchand, M.S. Minsky, S. Keller, P.T. Fini, J.P. Ibbetson, S.B. Fleischer, J.S. Speck, J.E. Bowers, E. Hu, U.K. Mishra, S.P. DenBaars, T. Deguchi, T. Sota, S. Nakamura, Appl. Phys. Lett. 74 (1999) 1460.
[6] Y. Kato, S. Kitamura, K. Hiramatsu, N. Sawaki, J. Crystal Growth 144 (1994) 133.
[7] P. Fischer, J. Christen, M. Zacharias, H. Nakashima, K. Hiramatsu, Solid State Phenomena 6 (1998) 151.
[8] J. Christen, M. Grundmann, D. Bimberg, J. Vac. Sci. Technol. B 9 (1991) 2358.
[9] F. Bertram, T. Riemann, J. Christen, A. Kaschner, A. Hoffmann, C. Thomsen, K. Hiramatsu, T. Shibata, N. Sawaki, Appl. Phys. Lett. 74 (1999) 359.
[10] A. Kaschner, A. Hoffmann, C. Thomsen, F. Bertram, T. Riemann, J. Christen, K. Hiramatsu, T. Shibata, N. Sawaki, Appl. Phys. Lett. 74 (1999) 3320.
[11] C. Fricke, R. Heitz, A. Hoffmann, I. Broser, Phys. Rev. B 49 (1993) 5313.
[12] L. Eckey, J. Holst, P. Maxim, R. Heitz, A. Hoffmann, I. Broser, B.K. Meyer, C. Wetzel, E.N. Mokhov, P.G. Baranov, Appl. Phys. Lett. 68 (1996) 415.
[13] E.I. Rashba, G.E. Gurgenishvili, Fiz. Tverd. Tela 4 (1962) 1095.
[14] J. Park, P.A. Grudowski, C.J. Eiting, R.D. Dupuis, Appl. Phys. Lett. 73 (1998) 333.